

Supporting Information

Facile Single-Step Synthesis of Ternary Multicore Magneto-Plasmonic Nanoparticles

Maria Benelmekki, Murtaza Bohra, Jeong-Hwan Kim, Rosa E.Diaz, Jerome Vernieres, Panagiotis Grammatikopoulos, Mukhles Sowwan

Nanoparticles by Design Unit, Okinawa Institute of Science and Technology (OIST) Graduate University, 1919-1 Tancha, Onna Son, Okinawa, 904-0495, Japan.

1. Deposition of the Ternary Fe-Ag@Si NPs

Nanoparticles were produced using a modified inert-gas condensation magnetron sputtering system (Figure S1). The principles of particle formation in inert gas condensation magnetron sputtering are well established ^[1,2]. In our experiments, a supersaturated vapor was generated by DC magnetron co-sputtering of high-purity Fe, Ag and Si targets mounted in a water-cooled aggregation chamber (labeled A). The sputtering conditions are described in the experimental section. Within this aggregation zone, nucleation of Fe, Ag and Si clusters took place in an inert gas atmosphere at a relatively high pressure, and was followed by the growth of larger ternary nanoparticles by coalescence. The pressure difference between the aggregation zone and the sample deposition chamber transported the freshly nucleated ternary nanoparticles through the differential-pumping aperture (Labeled B) and out of the aggregation zone to the deposition chamber (Labeled C). To increase the residence time of the NPs in the aggregation zone a flux of Ar gas can be introduced in differential-pumping aperture level as indicated in Figure S1. The nanoparticles were deposited on different types of substrates and TEM grids for further processing and characterization.

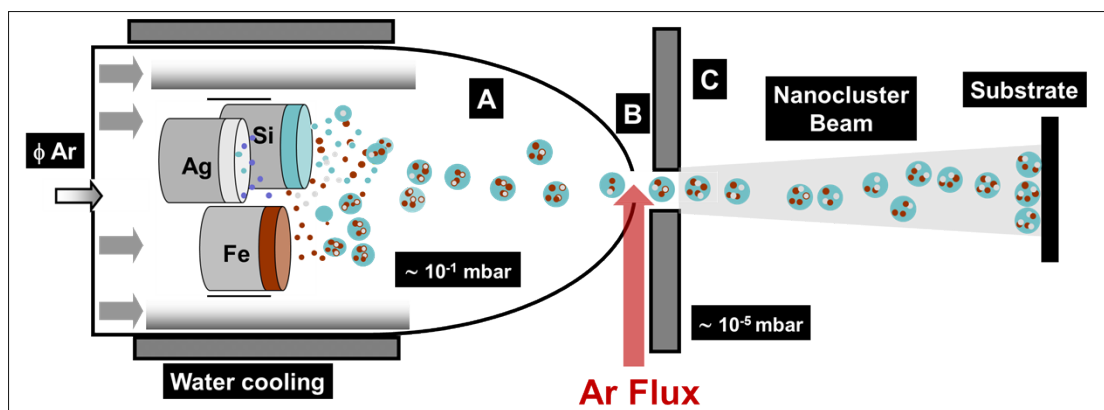


Figure S1. The co-sputter gas condensation system used for ternary NP deposition. Three high purity targets of Fe, Ag and Si, mounted in a water-cooled aggregation zone were simultaneously DC sputtered to create ternary hybrid nanoparticles composed of multiple dumbbell-like Fe-Ag cores encapsulated by a silicon (Si) shell.

2. Materials and Methods

One-inch pure Si (99.999%), Ag (99.99%) and Fe (99.9%) targets were used as sputtering materials. The power applied to the Si, Fe and Ag targets were 62 W and 9 W and 4.6 W respectively. The low power applied to the Ag is due to the high sputtering yield of Ag compared to Fe and Si [3]. The sputtering gas (Argon) flow was set at 55 sccm. During the deposition process, the pressure was $2.0 \cdot 10^{-1}$ mbar in the aggregation zone and $4.3 \cdot 10^{-4}$ mbar in the deposition chamber.

The nanoparticles were deposited on diced silicon substrates and carbon coated copper TEM grids for characterization. The working distances from the surface of the targets to the differential pumping aperture and from the differential pumping aperture to the substrate were ~ 20 cm and ~ 90 cm, respectively (Figure S1). For the Polyvinylpyrrolidone (PVP) film, a glass slide substrate (76 mm x 26 mm) was thoroughly cleaned in dry methanol for 10 min under ultrasonication, then dried under N_2 gas. 10 mg of PVP (Sigma-Aldrich, St. Louis, US) was dissolved in 250 μ L of methanol solution and gently dispensed onto the cleaned glass substrate. A thin PVP

film was formed by a spin-coater (MS-A-150, MIKASA, Japan) operated at 3,000 rpm for 30 sec. NPs were exfoliated by immersing the NPs/PVP/glass samples in methanol and sonicating for 15 min, followed by a separation step to remove the excessive PVP polymer using a centrifuge at 100,000 rpm for 60 min. After washing the precipitated NPs with methanol, the NPs were re-dispersed in ultrapure water from a Milli-Q system (Nihon Millipore K.K., Tokyo, Japan) using 0.1 μm filters.

TEM, STEM and EELS analysis were performed using a Cs-corrected-*FEI-Titan 80-300* kV operating at 300 kV. STEM and EELS analysis were performed with a camera length of 100mm and high energy resolution. SEM images were performed using a *FEI Quanta FEG 250* system. For XPS analysis, a *Kratos Axis UltraDLD 39-306* photoelectron spectrometer equipped with a mono $\text{AlK}\alpha$ source operated at 300 W was used. The field dependence of magnetizations curves (M-H loops) were measured with an in-plane sample configuration using a *Quantum Design Cryogen-Free Physical Property Measurement System (PPMS)*. UV-visible absorption spectra of nanoparticle suspensions were characterized using a *Thermo Scientific Multiskan GO UV-Vis* microplate spectrophotometer. The hydrodynamic radius of the nanoclusters was determined by dynamic light scattering (DLS) using a *Zetasizer Nano ZSP* (Malvern Instruments, Ltd.).

3-Modulating the size of the NPs

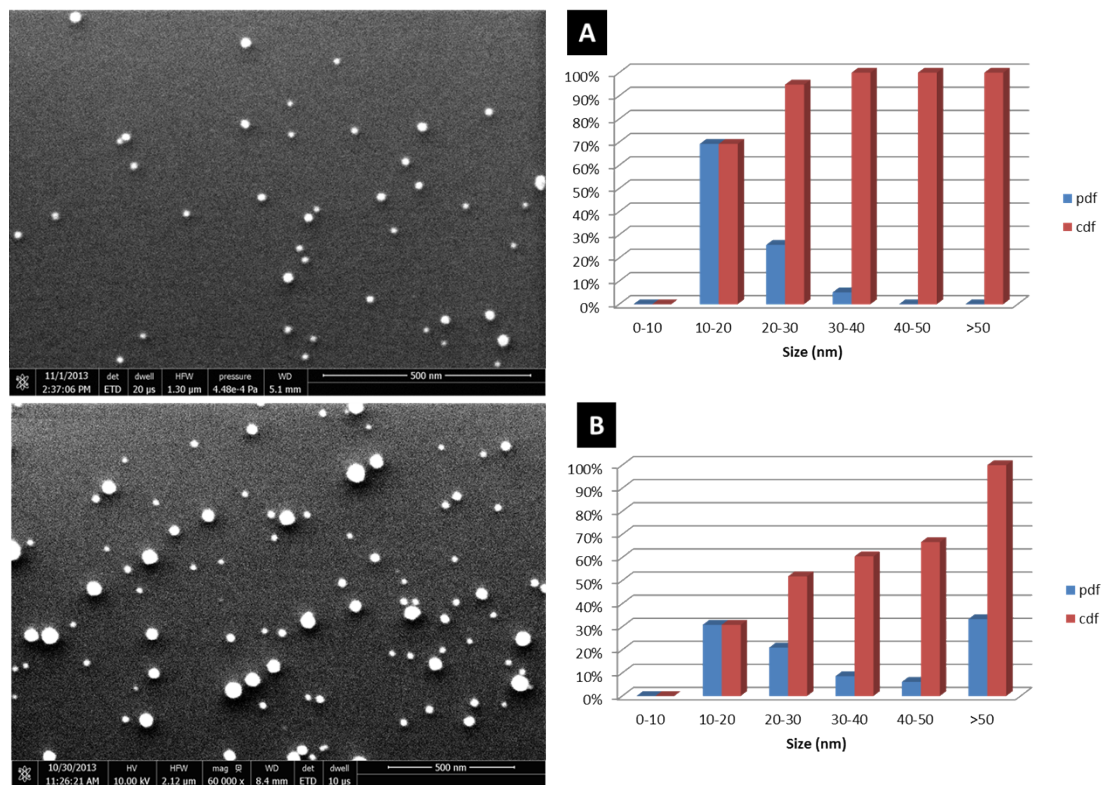


Figure S2. SEM images of The FeAg@Si nanoparticles deposited on Silicon substrate at 3.0×10^{-1} mbar of pressure at the aggregation zone. The pressure at the main chamber was increased from 7.5×10^{-4} mbar (A) to 3.9×10^{-3} mbar (B). The respective size probability distribution function (pdf), and cumulative distribution function (cdf) calculated over 85 imaged nanoparticles show that increasing the residence time of the NPs in the aggregation zone, leads to the formation of larger NPs.

4- Modulating the number of cores in each NP

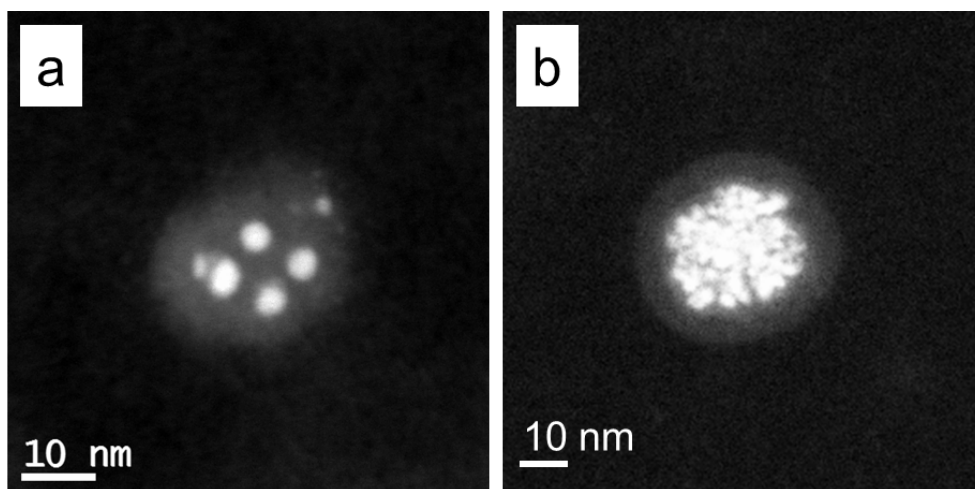
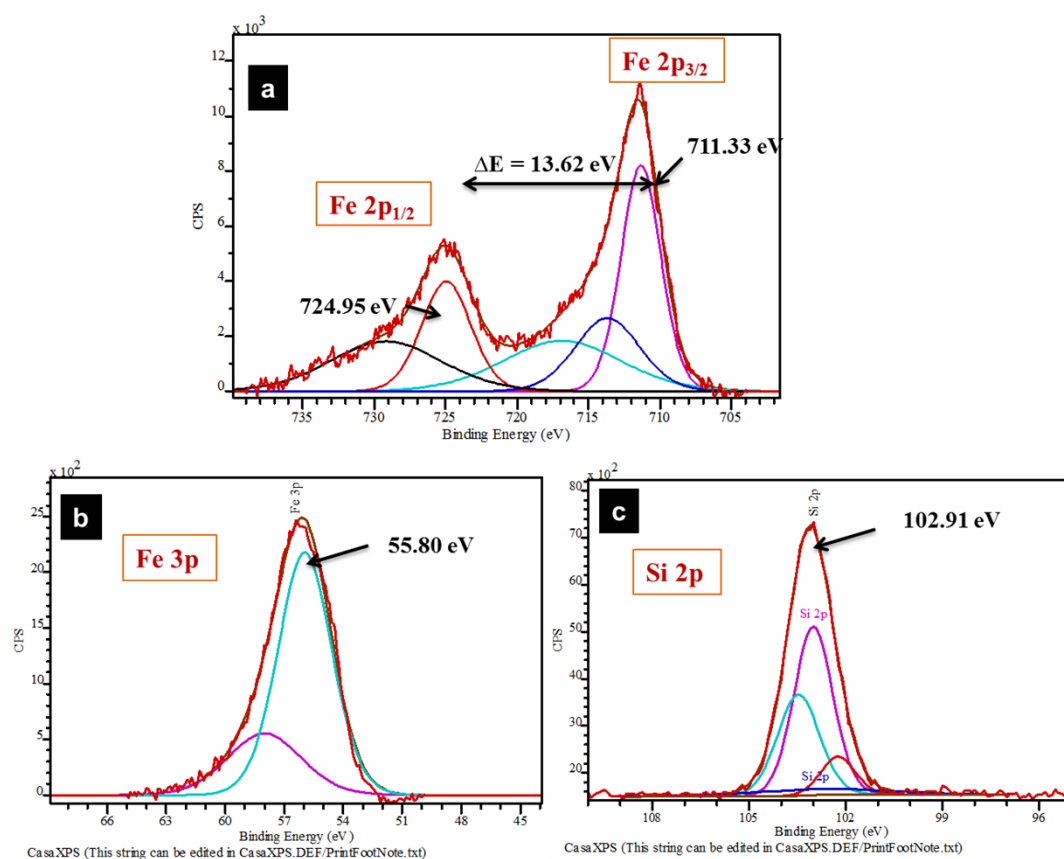


Figure S3. The number and size of cores in each nanoparticle can be altered by tuning the experimental conditions. For example (a) was obtained by applying 4.8W magnetron power on the Ag target under 7.5×10^{-4} mbar pressure in the deposition chamber and (b) was obtained by applying 6.7W magnetron power on the Ag target under 3.9×10^{-3} mbar pressure in the deposition chamber (keeping the powers on the Si and Fe fixed to 63W and 9W, respectively).

5-XPS measurements



Fi

Figure S4. XPS measurements on the Fe-Ag@Si nanoparticles. XPS spectra corresponding to Fe 2p (a) and Fe 3p (b) core levels from the FeAg@Si HNPs deposited on Si substrate. Spectra were resolved into their respective components by a mixed Gaussian–Lorentzian (GL, $m=30$) line-shape using commercial CasaXPS peak-fitting software. (a) The peak fitting for the Fe 2p_{3/2} core level at 711.33 eV indicates an Fe³⁺ oxidation state.^[4-6] Peak broadening near 718 eV may be attributed to either the Fe³⁺ satellite peak or to the overlap of Fe 2p_{3/2} and Ag 3s peaks.^[5] (b) Peak fitting for the Fe 3p core level shows a peak position at 55.8 eV, which is very close to the binding energy corresponding to the Fe³⁺ oxidation state. Broadening of the peak around 60 eV may be attributed to the overlap of Fe 3p and Ag 4p peaks.^[6,7] (c) Si 2p core level spectrum of an FeAg@Si nanoparticles deposited on Cu (100) single-crystal substrate. A broad peak centered at 102.91 eV was obtained, indicating full oxidation of the amorphous silicon shell.

6- UV-Vis UV-Vis spectra of Ag, Fe-Si and Si NPs.

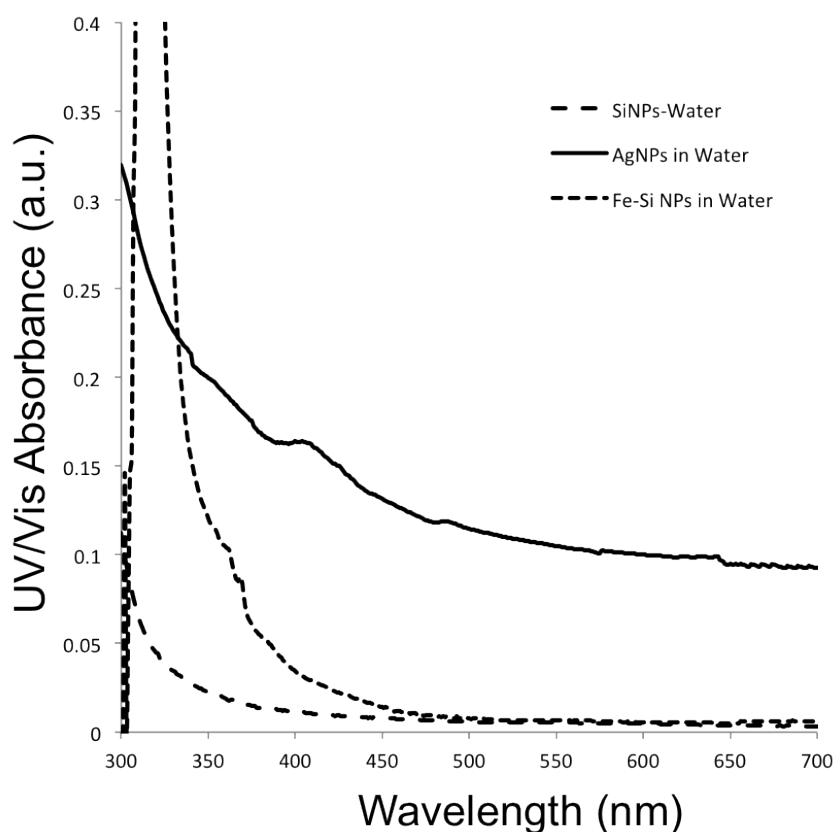


Figure S5. UV-Vis spectra of Ag, Fe-Si and Si NPs prepared under the same experimental conditions .

7- Mechanism of formation of the FeAg@Si NPs

Based on fundamentals of magnetron sputtering, and considering experimental conditions inside the aggregation zone (Figure S1A), we suggest a mechanism of formation of the FeAg@Si nanoparticles. In fact, when targets of Fe, Ag and Si are simultaneously sputtered, plasma density plays an important role in nucleation, growth, and crystallization of the nanoparticles. In the case of Ag targets, because of high sputtering yield (in our experimental conditions, ~ 1.20), electrons and ions are highly concentrated in the plasma region, inducing high-density plasma near the surface of the Ag target. In these conditions, nucleation and growth of the nanoparticles are completed before they leave the plasma zone. Then the

nanoparticles fly to the aggregation zone where the density of inert gas is sufficient to quench their high energy. As a result, particles keep their high temperature phase and larger nanoclusters with single crystalline structure are formed.

For Fe nanoparticles, the estimated sputtering yield is ~ 0.45 . Moreover, when the Fe target is loaded on the cathode, it provides an easy path for the magnetic flux generated by the permanent magnet of the cathode. Fluxes go through the Fe target and only a small portion is leaked out to help the generation of the magnetron plasma. Because plasma density and distribution are strongly correlated with magnetic field strength and the distribution of magnetic flux,^[10,11] during Fe sputtering, only a low concentration of electrons near the surface is obtained, and then the ionization rate is lower than with Ag targets, leading to a low density plasma. In this case, nucleation and growth of the nanoparticles occur when atoms fly into the aggregation zone (colder zone). Under these conditions, Fe atoms lose their energy rapidly and they form small, amorphous Fe nanoclusters.

Regarding Si nucleation and growth, as observed in HRTEM image (Figure 4a), the silicon shell presents an amorphous structure, suggesting its formation following the low density plasma mechanism. However, in this case, the low plasma density is attributed to the low sputtering yield of the silicon (~ 0.29). Sputtering yields were estimated using the simple sputtering yield calculator.^[12]

On the other hand, since nanocluster surfaces are not oxidized, the fractional number of surface atoms is very large. Then, in the aggregation zone, nanoclusters collide and coalesce with each other by diffusion of constituent atoms at their contact interfaces,

creating larger nanoparticles. This way, because of the large, positive free energy of Fe and Ag mixing, segregation of the elements forming core/shell or dumbbell-like structures is expected.^[8,9] However, from our TEM study, an almost exclusive formation of dumbbell-like structure was observed. A plausible explanation of this behavior is that when Fe and Ag nanoparticles collide in the aggregation zone, their energy is not enough to induce complete coalescence, so that only dumbbell-like structures are formed. Moreover, due to the low surface energy of amorphous silicon (1.05 J m^{-2}),^[13] Si clusters cover the surface of FeAg nanoparticles, resulting in a core/shell structure. Finally, during their flight along through aggregation zone, FeAg/Si core/shell nanoparticles collide and partially coalesce with each other resulting in multicore and irregular-shaped nanoparticles (FeAg@Si NPs).

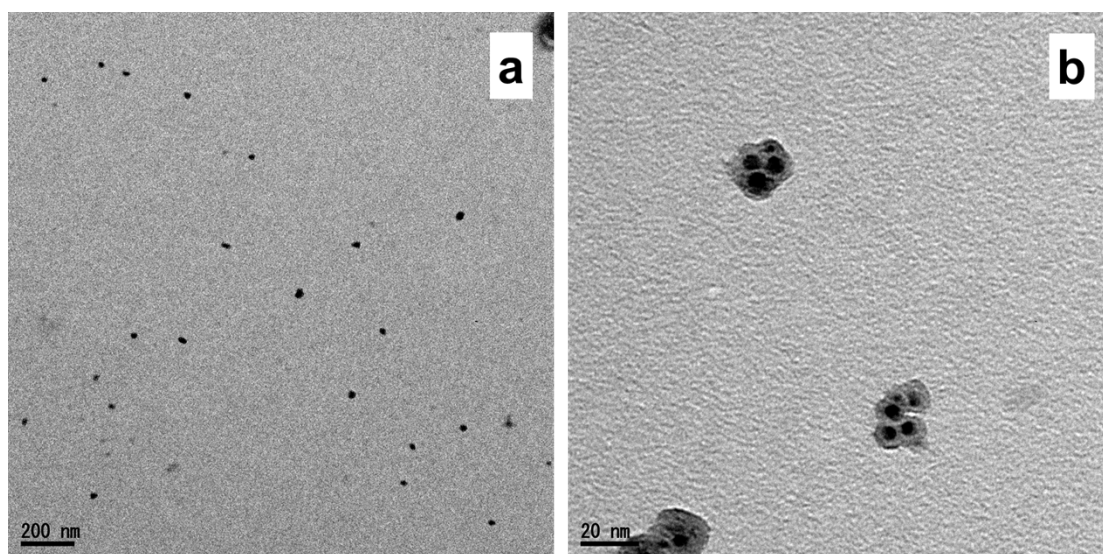


Figure S6. Low magnification TEM images of the obtained multicore nanoparticles.

References

- [1] H. Haberland, M. Karrais, M. Mall, Y. Thurner, *J. Vac. Sci. Technol. A* 1992, **10**, 3266-3271
- [2] K. Bromann, C. Félix, H. Brune, W. Harbich, R. Monot, J. Buttet, K. Kern *Science* 1996, **274**, 956-958.

- [3] S. Rosnagel, Handbook of Thin-Film deposition processes and techniques, **2002**, (Ed: K. Seshan) 319-348.
- [4] J.f. Moulder, w.f. Stickle, P.E. Sobol, K.D. Bomben “Handbook of X-ray photoelectron Spectroscopy” 1992, (Ed: J. Chastain). Perkin Elmer Corporation.
- [5] A.V. Mijiritskii, D.O. Boerma J. Mag. Mater. 2001, 232, 9-7
- [6] T. Yamashita, P. Hayes, App. Surf. Sci. 2008, 254, 2441-2449.
- [7] C.R. Brundle, T.J. Chuang, W. Wandelt, Surface Science 1977, 68, 459-468.
- [8] Y.H. Xu, J.P. Wang, Adv. Mater. 2008, 20, 994-999.
- [9] A. Elsukova, Z.A. Li, C. Möller, M. Spasova, M. Acet, M. Farle, M. Kawasaki, P. Ercius, T. Duden Phys. Status Solidi A 2011, 208, 2437-2442.
- [10] K. Nanbu, S. Kondo Jpn. J. Appl. Phys. 1997, 36, 4808-4814.
- [11] S. Ido, M. Kashiwawagi, M. Takahashi, Jpn. J. Appl. Phys. 1999, 38, 4450-4454.
- [12] www.iap.tuwien.ac.at/www/surface/sputteryield, “ A simple sputter yield calculator”, accessed October 2013.
- [13] S. Hara, S. Izumi, T. Kumagai, S. Sakai, Surface Science 2005, 585, 17-24.